Macromolecules
ARTICLE

Macromolecules **2009**, *42*, 7367–7378 **7367**
DOI: 10.1021/ma901247q

Exploration of Effective Catalysts for Diyne Polycyclotrimerization, Synthesis of an Ester-Functionalized Hyperbranched Polyphenylene, and Demonstration of Its Utility as a Molecular Container with Implication for Controlled Drug Delivery

Jianzhao Liu,[†] Li Zhang,[†] Jacky W. Y. Lam,*[,†] Cathy K. W. Jim,[†] Yanan Yue,[‡] Rui Deng,[‡] Yuning Hong,[†] Anjun Qin,[†,§] Herman H. Y. Sung,[†] Ian D. Williams,[†] Guochen Jia,[†] and Ben Zhong Tang*[,†,§]

[†]*Department of Chemistry, The Hong Kong University of Science & Technology (HKUST), Clear Water Bay, Kowloon, Hong Kong, China,* [‡]*Department of Chemistry, The Chinese University of Hong Kong (CUHK), Shatin, New Territories, Hong Kong, China, and* [§]*Department of Polymer Science and Engineering, Zhejiang University, Hangzhou 310027, China*

Received June 10, 2009; Revised Manuscript Received August 21, 2009

ABSTRACT: We present the first examples of a group of effective ruthenium catalysts for polycyclotrimerization. The polymerization reactions of an arylene bipropiolate monomer initiated by the Ru(II−IV) complexes of $CpRu(PPh_3)_2Cl$, $Cp^*Ru(PPh_3)_2Cl$, $[Cp^*RuCl_2]_n$, and $[Ru(\eta^3{:}\eta^3\text{-}C_{10}H_{16})(\mu\text{-}Cl)Cl]_2$ (Cp = cyclopentadienyl, Cp* = pentamethyl-Cp, and $C_{10}H_{16}$ = 2,7-dimethylocta-2,6-diene-1,8-diyl) produce ester-functionalized poly(aroxycarbonylphenylene) (PACP) with high molecular weights (M_w up to 200×10^3) in good yields (up to 90%). Topological structure of the polymer product can be hyperbranched or cross-linked, tunable by the extent of triple-bond conversion. The degree of branching (DB) of the PACP is ~0.76, much higher than those of the "conventional" hyperbranched polymers (DB ~ 0.5). The PACP exhibits high transparency in the visible spectral region. It works as a molecular container, effectively trapping small molecules in its cavities with the aid of hydrogen-bond interaction. The polymer undergoes a bursting hydrolysis reaction, and the collapse of its hyperbranched skeleton rapidly releases the loaded molecules, showing promise as a drug carrier for missile therapy.

Introduction

The past decades have witnessed remarkable progress in the area of research on hyperbranched polymers.[1] Because of their unique size-, shape-, and surface-specific properties, hyperbranched polymers have found an array of novel applications in a diversity of areas including chemical sensing, micellar mimetic, gene delivery, supramolecular assembly, and molecular antenna systems. To further advance the area of research and to realize full potential of hyperbranched polymers, it is important to develop versatile synthetic methods for making hyperbranched polymers. The methodologies currently available for synthesizing hyperbranched polymers are rather limited. The commonly taken synthetic approaches have been the polymerizations of single-component AB_n ($n \geq 2$)-type and binary-component $A_2 + B_n$ ($n \geq 3$)-type monomers. The former approach, however, suffers from such drawbacks as the synthetic difficulty in the monomer preparation and the self-oligomerization problem during the monomer storage due to the coexistence of two mutually reactive functional groups in one monomer structure, while the latter approach requires stoichiometric balance of the two monomers in order to produce polymers with high molecular weights (MWs) and degrees of branching (DBs). Polycyclotrimerization of A_2-type diynes is free of the shortcomings discussed above and is emerging as a versatile and atom-economical approach to functionalized hyperbranched polymers.[2]

The A_2-type approach offers the opportunity to tune topological structure of the polymeric product. Whereas vinyl polymerizations of diene monomers generally result in the formation of cross-linked polymers, molecular structures of the polymers synthesized from acetylenic polymerizations of diyne monomers can be hyperbranched or cross-linked, depending on the extent of triple-bond conversion (p). From a pure structural point of view, we have derived a simple mathematical formula that gives a critical extent of conversion (p_c) of ~75%, at which a structural transition from hyperbranched polymer to cross-linked gel occurs.[3] The kinetic model built by Irzhak et al. predicts p_c values of 0.50 and 0.62 under different conditions.[4] Use of a diluter reaction solution favors the formation of hyperbranched polymer and can shift the gel point to a higher conversion ($p_c > 0.62$). The interbranch reactions can be restricted to within a polymer sphere through the manipulation of reaction conditions and optimization of process parameters. As a result, no gelation occurs even at very high p values, as the main products are soluble nanogels with interbranch loops of different sizes but minimal extents of intersphere cross-links.[5]

Our research groups have worked on polycyclotrimerizations for many years and have developed several transition-metal catalysts for the polymerizations of diyne monomers.[2] We have synthesized a number of hyperbranched polyarylenes by the tantalum-, niobium-, and cobalt-catalyzed [2 + 2 + 2] alkyne cyclotrimerizations and found that the polymers exhibit an array of unique properties, such as efficient fluorescence (quantum yield up to 98%), fast photoresponse, excellent thermal stability (T_d up to 600 °C), and strong optical nonlinearity.[6] The Ta- and Nb-based catalysts, however, show little tolerance to functional groups. Although the Co catalysts can polymerize diyne monomers containing certain polar moieties, the catalysts need to be activated by UV irradiation and the resultant polymers generally

*Corresponding authors. E-mail: chjacky@ust.hk (J.W.Y.L); tangbenz@ust.hk (B.Z.T.).

Published on Web 09/04/2009

Scheme 1. Ru-Catalyzed Polycyclotrimerization of an ABP Monomer

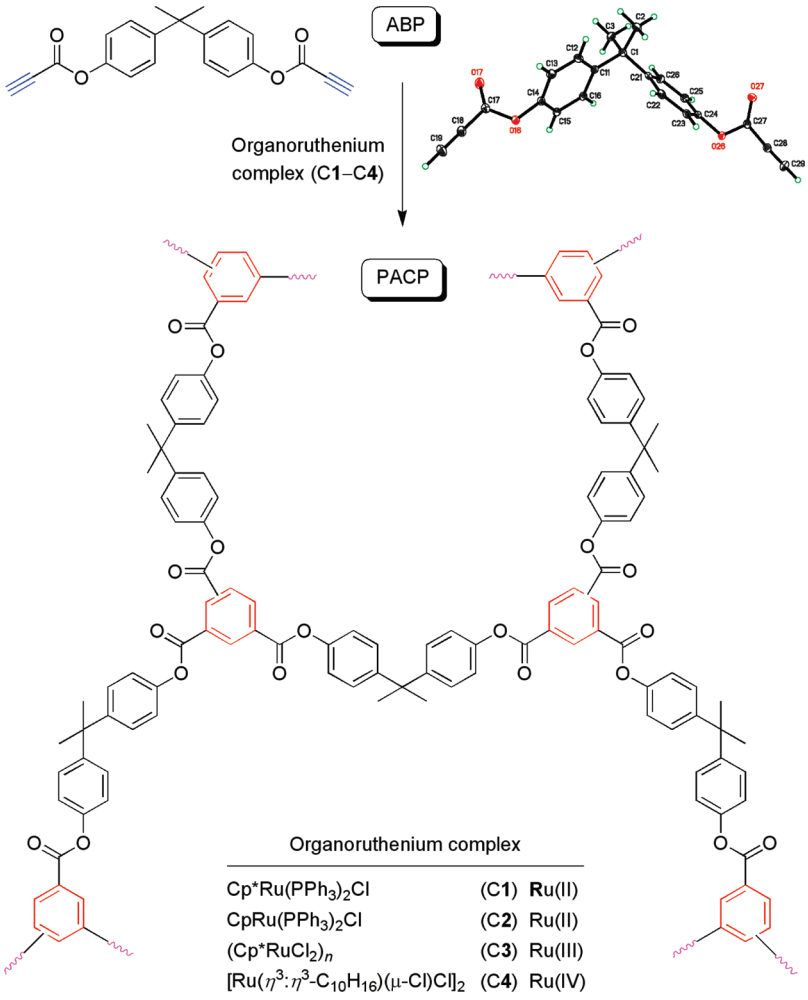

Scheme 2. Synthesis of Ester-Functionalized Diyne Monomer

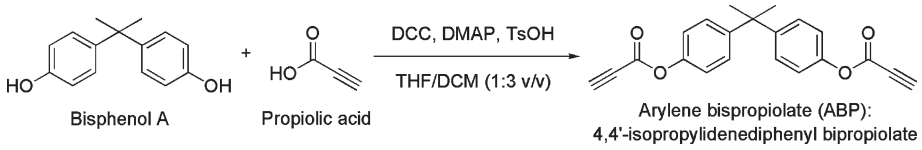

have lower MWs and show inferior optical and photonic properties than the polymers prepared by the Ta and Nb catalysts.[7] This calls for the exploration of new catalyst systems with improved performances, especially higher tolerance to functional groups.

With this in mind, we turn our attention to ruthenium complexes. Ru is a late transition metal and is electron-richer than its early transition metal counterparts of Ta and Nb. Its complexes are therefore expected to show higher tolerance to polar functional groups. While many research groups have used Ru complexes as catalysts for alkyne cyclotrimerizations in the transformations of small molecules,[8,9] their utilization as catalysts for alkyne polycyclotrimerization has been virtually unexplored. In this work, we developed a series of organoruthenium complexes with oxidation states ranging from II to IV (**C1**−**C4**)[10−13] into effective catalysts for the polymerization of an arylene bispropiolate (ABP) monomer (Scheme 1). The Ru-catalyzed polycyclotrimerizations yielded soluble poly(aroxycarbonylphenylene)s (PACPs) with high MWs and hyperbranched or cross-linked structures. The hyperbranched polymers effectively trapped small molecules in their internal cavities via noncovalent interactions and quickly released the loaded molecules through a bursting hydrolysis. In this paper, we report the synthesis and characterization of the PACPs and demonstrate their potential as molecular containers for controlled drug delivery.

Results and Discussion

Polymer Synthesis. The ABP monomer used in this study, 4,4′-isopropylidenediphenyl bipropiolate, was readily prepared by a one-step, one-pot reaction of bisphenol A with propiolic acid, in the presence of 1,3-dicyclohexylcarbodiimde (DCC), 4-(dimethylamino)pyridine (DMAP), and *p*-toluenesulfonic acid monohydrate (TsOH) in a tetrahydrofuran (THF)/dichloromethane (DCM) mixture (Scheme 2). The diyne monomer was thoroughly purified and fully characterized by spectroscopic and crystallographic methods, from which satisfactory analysis data corresponding to its expected molecular structure were obtained (see Experimental Section for detailed characterization data and Table S1 in the Supporting Information for the crystal analysis data).

Scheme 3. Proposed Mechanism for Ru-Catalyzed Diyne Polycyclotrimerization

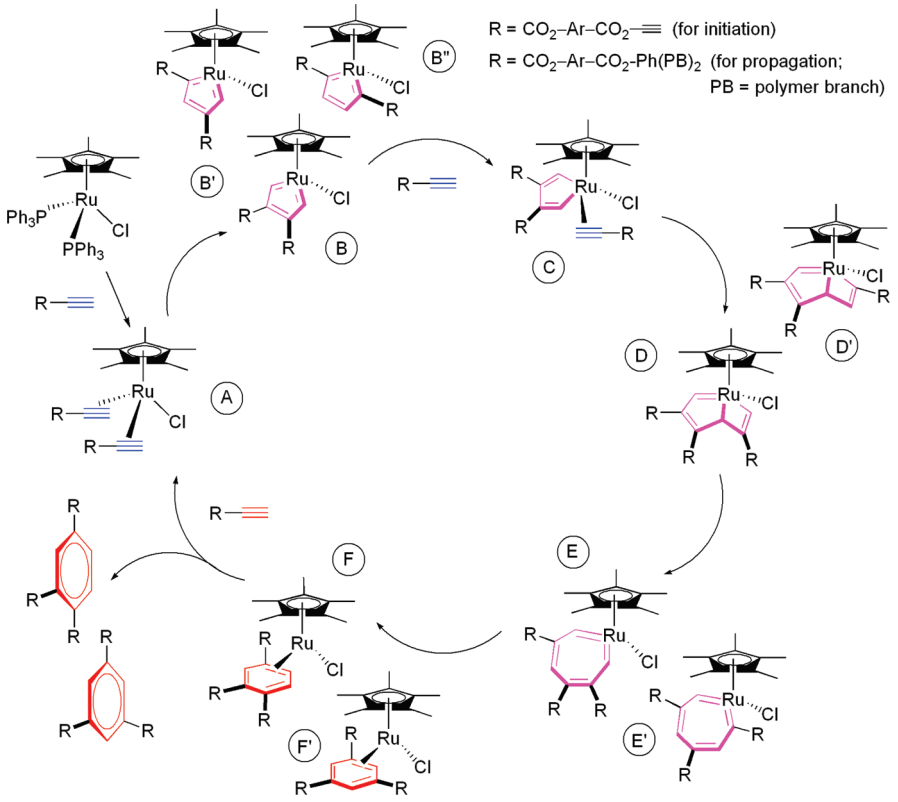

Table 1. Polycyclotrimerizations of the Diyne Monomer Catalyzed by the Ru(II) Complexes[a]

no.	solvent	[cat.] (mM)	time (h)	yield (%)	p (%)[b]	S[c]	$M_{w,r}$[d]	$M_{w,a}$[e]	PDI[d]
				Catalyst C**1**					
1	toluene	1	1	76.4		×			
2	DCM	1	1	100		×			
3	DCE	1	1	68.6		√	6000		1.8
4	dioxane	1	1	49.4		√	4200		1.5
5	THF	1	1	62.1	69.4	√	6400	80000	1.9
6	THF	1	2	83.2	73.9	√	12100	120000	2.5
7	THF	1	3	87.8		√	23300	190000	2.9
8	THF	1	4	90.3	88.5	√	27400	200000	3.5
9	THF	1	6	89.2		×			
10	THF	2	1	72.4		√	8400		2.0
11	THF	5	1	68.6		×			
12	THF/H_2O[f]	1	1	77.6		√	7100		2.0
13	THF/H_2O[f]	1	2	84.8		√	8000		2.2
				Catalyst C**2**					
14	THF	1	8	30.3		√	5000		1.7
15	DCM	1	8	33.3		√	4600		1.7
16	DCM	2	0.5	79.6		√	8200		2.0

[a] Carried out under nitrogen at room temperature and 75 °C using C**1** and C**2** as catalysts, respectively; $[M]_0$ = 0.1 M. Abbreviations: DCM = dichloromethane, DCE = 1,2-dichloroethane, and THF = tetrahydrofuran. [b] Extent of triple-bond conversion. [c] Solubility (S) tested in common organic solvents such as THF, chloroform, and DCM; √ = completely soluble, × = insoluble. [d] Relative weight-average molecular weight ($M_{w,r}$) and polydispersity index (PDI) estimated by gel-permeation chromatography (GPC) in THF on the basis of a linear polystyrene calibration. [e] Absolute weight-average molecular weight ($M_{w,a}$) determined by static laser light scattering technique (LLS). [f] Volume ratio of THF:H_2O = 9:1.

We systematically studied the polycyclotrimerizations of the ABP monomer catalyzed by the Ru(II−IV) complexes. Table 1 lists the results of its polymerizations in the presence of Ru(II) complexes of Cp*Ru(PPh_3)$_2$Cl (C**1**) and CpRu(PPh_3)$_2$Cl (C**2**). While insoluble gels are formed when the reactions are catalyzed by C**1** in toluene and DCM, completely soluble polymers are obtained in high yields from the polymerizations conducted in DCE, dioxane, and THF, with the reaction in THF giving a polymer with the highest MW (Table 1, nos. 3−5). The time-course study of the reaction in THF reveals that prolonging the polymerization time from 1 to 4 h results in increases in the extent of triple-bond conversion (p up to 88.5%) and the yield (up to ~90%) and MW ($M_{w,a}$ up to 200 × 10^3) of the polymer (Table 1, nos.

Table 2. Polycyclotrimerizations of the Diyne Monomer Catalyzed by the Ru(III) and Ru(IV) Complexes[a]

no.	$[M_0]$ (M)	temp (°C)	time (h)	yield (%)	*S*	$M_{w,r}$	PDI
			Catalyst C**3**				
1	0.1	75	0.5	75.0	×		
2	0.05	rt	0.1	73.2	×		
3	0.05	0	3.0	61.2	√	5800	1.9
			Catalyst C**4**				
4	0.1	rt	48	0			
5	0.1	75	1	36.4	√	4700	1.8
6	0.1	75	3	56.1	√	5400	2.0

[a] Carried out in THF under nitrogen; for nos. 1−3: [cat.] = 1 mM; for nos. 4−6: [cat.] = 5 mM. For definitions of the abbreviations, see the footnotes of Table 1.

5−8). Cross-linked networks, however, are formed when the reaction time is further lengthened.

It is noteworthy that the polymer product obtained at a *p* value as high as 88.5% is still completely soluble in common organic solvents. The solubility of the polymer suggests that it is a nanogel with intrasphere loops and with a few, if any, intersphere cross-links. Increasing the catalyst concentration accelerates the polymerization reaction. No soluble polymers are obtained if the concentration becomes too high (Table 1, no. 11). Intriguingly, high-MW polymers are produced in a THF/H_2O mixture, with the polymer yields being even higher than those obtained from the reactions carried out in pure THF. Water may have served as a cocatalyst in the polymerization system. The exact role of water in the polymerization system is unclear at present and is under investigation in our laboratories. The catalytic activity of C**2** is generally lower than that of C**1**, as can be understood from the data shown in Table 1 (cf. nos. 2, 5, and 14−16).

The Ru-catalyzed diyne polycyclotrimerization may have proceeded through a metallacycle route (Scheme 3).[8,14,15] In the catalytic cycle, the phosphine ligands of the Ru complex are replaced by two triple bonds from two diyne monomers in the initiation step or two growing "repeat branches" in the propagation step. Oxidative cyclization of the triple bonds on the low-valent Ru metal center gives metallacyclopentatrienes B. Insertion of another triple bond gives metallacycles D and E, and reductive elimination followed by dissociation affords the trisubstituted benzene rings or the new repeat branches in the hyperbranched polymer. The oxidative cyclization is a rate-determining step in the whole catalytic cycle. In comparison to Cp ring, Cp* ring is sterically bulkier and electronically richer. The oxidative cyclization thus should occur more readily in the system of C**1** because of easier dissociation of its PPh_3 ligands. Whereas the [CpRuCl] fragment of C**2** may coordinate with the newly formed benzene ring to give a stable sandwich η^6 complex to break down the catalytic cycle, this coordination process is difficult for [Cp*RuCl] of C**1** due to the steric effect of its bulkier Cp* ring. The [Cp*RuCl] fragment of C**1** is more readily regenerated,[11,12] which keeps the catalytic cycle running smoothly, thus resulting in the formation of a polymer with a higher MW in a higher yield.

Interestingly, high-valent Ru complexes C**3** and C**4** can also catalyze the diyne polycyclotrimerization (Table 2). The catalytic activity of C**3** is higher than those of C**1** and C**2**, as can be understood from the fast rate of the reaction it initiates: an insoluble gel is formed in as short as 0.1 h even when the reaction is conducted at a lower monomer concentration at a lower temperature (room temperature). Completely soluble polymer, however, is obtained by further decreasing the reaction temperature (Table 2, no. 3). This is the first example of using a Ru(III) complex as catalyst for polycyclotrimerization. Complex C**3** may have readily disproportionated to generate Ru(II) and Ru(IV) species in the presence of the diyne monomer. The polycyclotrimerization then quickly proceeds to give cross-linked gels in the presence of the active Ru(II) species. Since C**4** is a chloro-bridged bis(allyl)ruthenium(IV) dimer, the reactions are carried out at an elevated temperature in order to provide sufficient energy to dissociate the bisallyl diradical to active Ru(II) species.[9] Catalysts C**3** and C**4** are easy to prepare and very stable. We are now further exploring their utility for the synthesis of other functionalized acetylenic polymers.

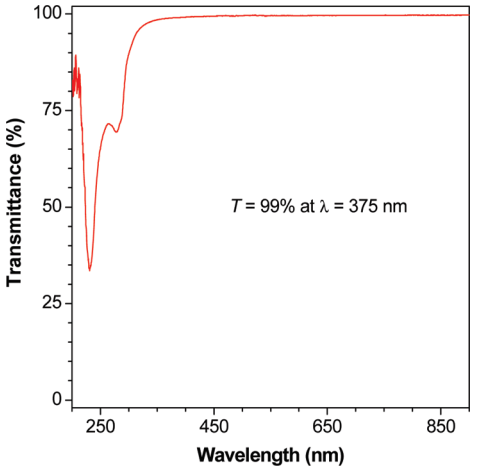

Figure 1. Transmission spectrum of a THF solution (10 μM) of PACP (sample taken from Table 1, no. 6).

The hyperbranched polymers are soluble in common organic solvents, such as DCM, chloroform, and THF, and are thermally stable, showing degradation temperatures of ~300 and ~280 °C in air and under nitrogen, respectively (Supporting Information, Figure S1). The PACP is highly transparent in the visible spectral region, absorbing little light (≤1%) at wavelengths longer than 375 nm (Figure 1). The polymer is thus a promising candidate material for photonic applications.[16] This excellent optical transparency is due to its hyperbranched structure and ester linkage: the former prevents aggregation of the aromatic rings between the polymer molecules, and the latter weakens electronic communication between the aromatic rings inside a polymer molecule and decreases the extent of $\pi-\pi$ conjugation.

Structural Characterization. The polymer structure is characterized by spectroscopic methods with satisfactory results (see Experimental Section for detailed analysis data). The IR spectrum of PACP is shown in Figure 2; the spectrum of its monomer is also given in the same figure for the purpose of comparison. The strong absorption band observed at 3268 cm^{-1} in the spectrum of the diyne monomer is associated with its ≡C−H stretching vibration. This band becomes weaker in the spectrum of the polymer, indicating that most of the diyne triple bonds have been consumed by the polymerization reaction. The C≡C stretching vibration of the monomer at 2126 cm^{-1} is also decreased considerably after polymerization.

Figure 3 shows the ^1H NMR spectra of the polymer as well as its monomer. The peak at δ 3.14 in the spectrum of the monomer due to the resonance of its acetylene proton is dramatically weakened in the spectrum of the polymer, confirming that a large fraction of the triple bonds has been consumed by the polycyclotrimerization reaction. The unreacted triple bonds are located at the peripheries of the

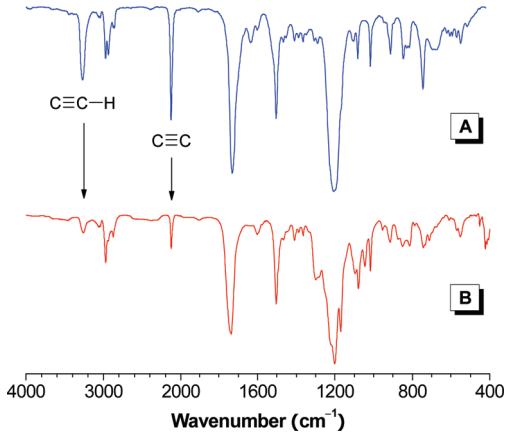

Figure 2. IR spectra of (A) the diyne monomer and (B) its polymer (sample taken from Table 1, no. 6).

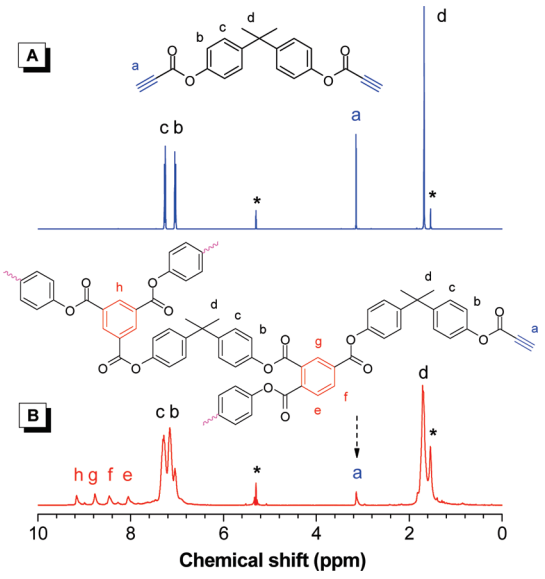

Figure 3. ^{1}H NMR spectra of (A) the diyne monomer and (B) its polymer (sample taken from Table 1, no. 6) in DCM-d_2. The solvent peaks are marked with asterisks.

polymer as terminal groups and embedded inside the polymer sphere as part of its linear component. The polymer shows broader and stronger resonance peaks in the aromatic region than its monomer. New resonance peaks are emerged in the downfield region ($\delta \sim 8.0-9.2$). Through comparison with those of the model compound prepared by the cyclotrimerization of methyl propiolate (Figure 4), it is clear that the triple bonds of the diyne monomer have been cyclotrimerized into 1,2,4/1,3,5-trisubstituted benzene rings of polyphenylene. Calculations of the isomeric ratios of the products obtained from the monoyne cyclotrimerization and the diyne polymerization reveal that the reactions proceed in a regioselective fashion, giving 1,2,4-trisubstituted benzene isomer as the main product ($F_{1,2,4}$ up to 80%; Table 3).

The ^{13}C NMR spectrum of the polymer shows weak resonance peaks of acetylenic carbon atoms at δ 77.1 and 74.7, with new peaks appearing in the aromatic-carbon resonance region (Figure 5B). All the resonance peaks are readily assignable, as clearly marked by letters a−m in the figure, with no strange peaks detected, indicative of the high purity of the polymer product. The ^{1}H{^{13}C} heteronuclear single quantum coherence (HSQC) spectra further prove the structure of the polymer. ^{1}H{^{13}C} HSQC spectra are a

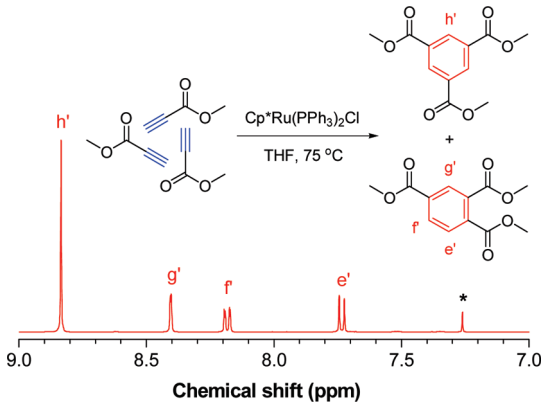

Figure 4. ^{1}H NMR spectrum of chloroform-*d* solution of an isomeric mixture of trimethyl 1,3,5/1,2,4-benzenetricarboxylates prepared from model cyclotrimerization reaction of methyl propiolate catalyzed by C**1** (sample taken from Table 3, no. 1). The solvent peak is marked with an asterisk.

Table 3. Synthesis and Regioselectivity of Ru-Catalyzed (Bi)propiolate (Poly)cyclotrimerization[a]

no.	catalyst	yield (%)	$F_{1,2,4}$ (%)[b]
	Cyclotrimerization		
1	C**1**	87.3	56.5
2	C**3**	86.1	77.7
3	C**4**	70.2	66.7
	Polycyclotrimerization[c]		
4	C**1**	83.2	80.8
5	C**3**	61.2	75.0
6	C**4**	56.1	70.6

[a] Carried out in THF under nitrogen for 24 h at 75 °C (for nos. 1 and 3) or at room temperature (for no. 2); $[M]_0 = 0.5$ M. [b] Calculated from $F_{1,2,4} = A_{1,2,4}/(A_{1,2,4} + A_{1,3,5})$, where A is the integrated peak area of the proton resonance of the newly formed benzene ring. [c] Samples for nos. 4−6 were from Table 1, no. 6 and Table 2, nos. 3 and 6, respectively.

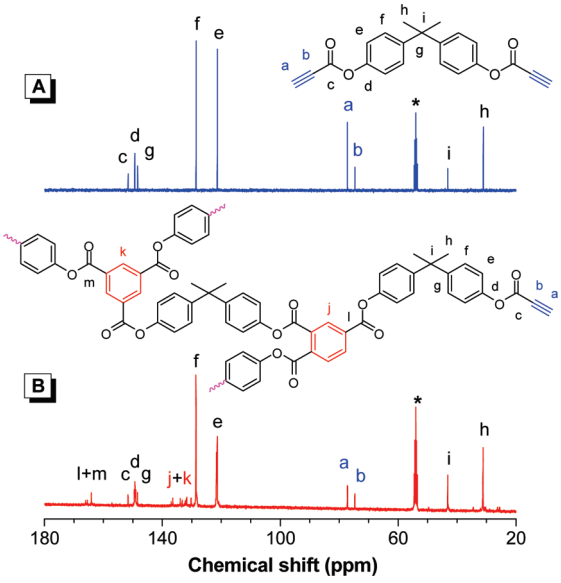

Figure 5. ^{13}C NMR spectra of (A) the diyne monomer and (B) its polymer (sample taken from Table 1, no. 6) in DCM-d_2. The solvent peaks are marked with asterisks.

powerful NMR analytical technique that can provide information on one bond C−H coupling, which gives cross-peaks between the signals of each unique proton and its directly

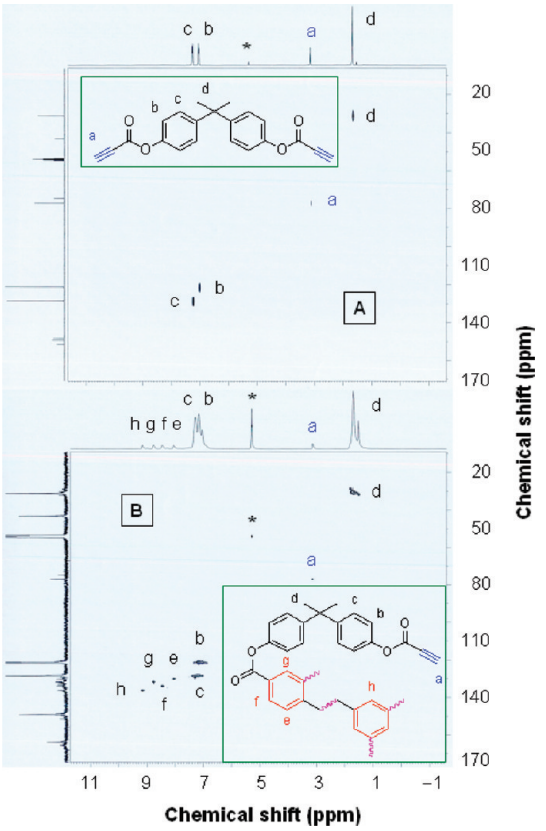

Figure 6. $^1H\{^{13}C\}$ HSQC NMR spectra of (A) the diyne monomer and (B) its polymer (sample taken from Table 1, no. 6) in DCM-d_2. The solvent peaks are marked with asterisks.

attached carbon atom. By comparison with the spectrum of the diyne monomer, it is evident that four new cross-peaks appear in the spectrum of the polymer (Figure 6B), which correspond very well to the C−H bonds in the newly formed 1,2,4- and 1,3,5-trisubstituted benzene rings via alkyne cyclotrimerization. All these spectral data substantiate that many of the diyne triple bonds have been transformed into benzene rings by the polycyclotrimerization reaction.

DB and Degree of Polymerization (DP_n). We normally terminate a polycyclotrimerization reaction before it reaches gel point (p_c) in order to obtain soluble hyperbranched polymer. To estimate the p_c value, we need to revisit the relationship between the topological structure of the polymer and the extent of triple-bond conversion (p). In our previous paper, from a pure structure viewpoint, we have deduced that if no loops are formed in the diyne polycyclotrimerization, the upper limit of p value or p_c is 75%.[3] On the basis of a kinetic model, Irzhak et al. conducted theoretical studies on polycyclotrimerization and predicted that the p_c values were 0.50 and ~0.62, respectively, with nonallowance and allowance for the first shell negative substitution effect, that is, the decrease in the reactivity of the second functional group in the monomer after the transformation of the first functional group by the polymerization.[4]

From the ^1H NMR spectrum shown in Figure 3B, the p value in our diyne polycyclotrimerization system can be estimated from eq 1:

$$p = \frac{N_{RT}}{N_{TT}} = \frac{A_f}{\frac{A_0}{8} \times 2} = \frac{4A_f}{A_0} \quad (1)$$

where N_{RT} is the number of reacted triple bonds, N_{TT} is the total number of triple bonds of the monomer molecules, and

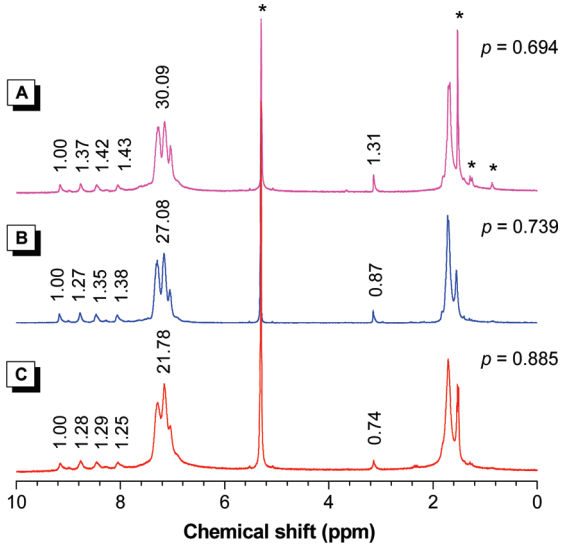

Figure 7. ^1H NMR spectra of DCM-d_2 solutions of the polymers obtained from the time-course study at specified periods of polymerization time: (A) 1 h, (B) 2 h, and (C) 4 h (samples taken from Table 1, nos. 5, 6, and 8, respectively). The peaks for solvent, water, and petroleum ether are marked with asterisks.

A_0 and A_f are the integrated areas of resonance peaks of the protons of the original and newly formed benzene rings, respectively. The p values are calculated for the polymers obtained from the time-course study, which are 0.694, 0.739, and 0.885 at the polymerization times of 1, 2, and 4 h, respectively (Figure 7 and Table 1, nos. 5, 6, and 8). From the models discussed above,[3,4] cross-linking reaction must occur to render the product insoluble after 4 h polymerization. Surprisingly, however, all the polymers are completely soluble, with no insoluble gels formed. The dilute monomer solutions we used in the polycyclotrimerization reactions must have helped shift the gel point to a high p value (p_c > 0.62). When the p value is smaller than 0.75, the probability for the loop formation is low and the polymers possess a hyperbranched topological structure, whereas when p is larger than 0.75, some intrasphere loops and a few intersphere links may be formed. The polymers thus have been cross-linked or gelled, but their tiny sizes make the polymer nanogels still completely soluble in common organic solvents.[17]

In order to simplify the structural analysis, it is assumed that no loops are formed in a polymer when $p < 0.75$. On the basis of this postulation, the relationships between p and the number of newly formed benzene rings (N_b) and between DP_n and N_b are established, as given in eqs 2 and 3, respectively.[3]

$$p = \frac{3N_b}{4N_b + 2} \quad (2)$$

$$DP_n = 2N_b + 1 \quad (3)$$

According to eqs 2 and 3 when p is 0.739, N_b and DP_n are equal to 33.6 and 68.2, respectively. From eq 4, the number-average MW of the polymer (M_n) is calculated to be

$$M_n = DP_n \times M_m = 2.27 \times 10^4 \quad (4)$$

where M_m is the MW of the monomer. Comparing the calculated M_n value with that estimated by GPC relative to the polystyrene standards (eq 5), the difference is as large as

Scheme 4. AIE Luminogen-Loaded Hyperbranched Polymer PACP−BCTPE and Its Bursting Hydrolysis

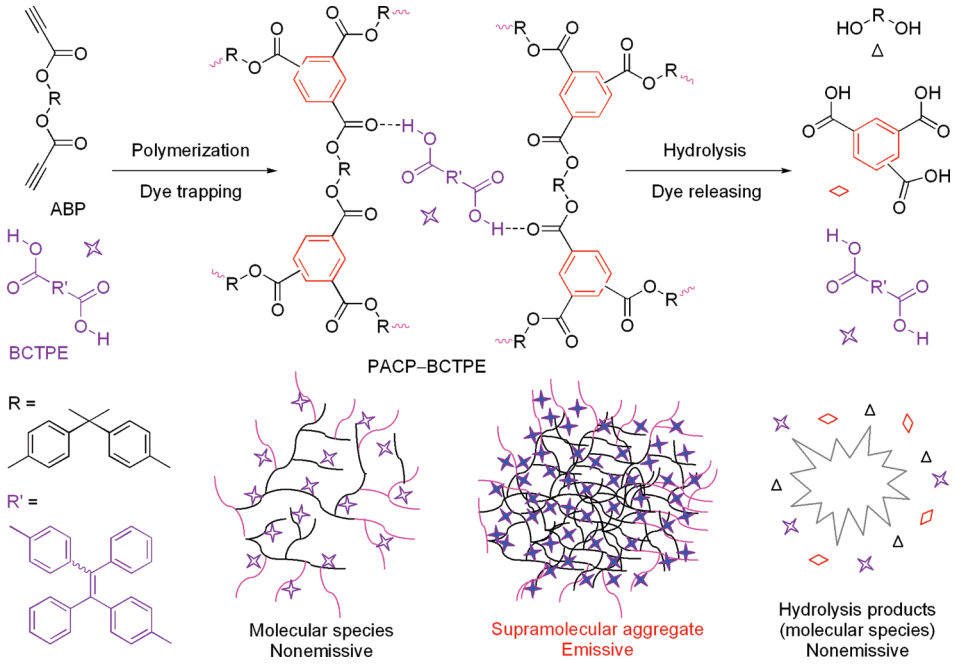

4.73 times due to the globular architecture of the hyperbranched polymer.[18]

$$r = \frac{M_{n,\mathrm{NMR}}}{M_{n,\mathrm{GPC}}} = \frac{22700}{4800} = 4.73 \qquad (5)$$

The measurement of the $M_{w,a}$ values by the LLS technique provides solid evidence to further prove the globular architecture of the hyperbranched polymer. The $M_{w,a}$ values are ~7−13 times higher than those estimated by GPC (Table 1). It thus becomes clear that the Ru-catalyzed diyne polycyclotrimerization can produce polymers with high MWs ($M_{w,a}$ up to 200×10^3) in short periods of polymerization time. The high efficiency and great functionality tolerance of this catalyst system have enabled the synthesis of functionalized hyperbranched polymers through the A_2-type construction route.

Because of the difficulty in differentiating the terminal unit from the linear unit in a hyperbranched polymer from diyne polycyclotrimerization by spectroscopy techniques, we have derived some simple mathematic equations for DB calculation in our previous work.[3] From the conclusion given in eq 6 and the definition given in eqs 7 and 8,[1] we get eq 9:

$$\frac{2f_T + f_L}{f_T - f_D} = \mathrm{DP}_n(1-p) \qquad (6)$$

$$\mathrm{DB} = \frac{f_T + f_D}{f_T + f_D + f_L} \qquad (7)$$

$$f_D + f_T + f_L = 1 \qquad (8)$$

$$\mathrm{DB} = 2f_D + \frac{1}{\mathrm{DP}_n(1-p)-1} = 2f_D + 0.06 \qquad (9)$$

where f_D, f_T, and f_L are the fractions of the D, T, and L units, respectively (Chart 1). According to the result of our previous structural modeling study,[3] the f_D value is estimated to be close to or higher than 0.3, which means that at least 3 out of 10 newly formed benzene rings are the dendritic units. The

Chart 1. Generalized Basic Structural Units in Hyperbranched PACP

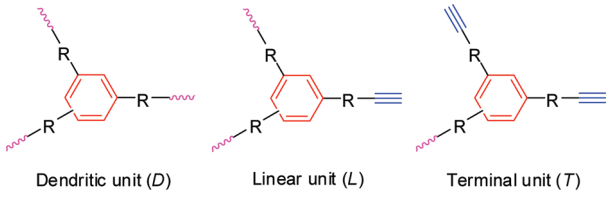

DB value is thus about 0.76, much higher than those of the "conventional" hyperbranched polymers prepared by the polycondensations of AB_2-type monomers (DB ~ 0.5). When the negative substitution effect was taken into account, Irzhak et al. theoretically deduced a DB value of ~0.71 at the critical gel point,[4] in reasonable agreement with our experimental result.

Molecular Container. Since Meijer and co-workers demonstrated the dendritic box about 15 years ago, many research groups have studied the molecular encapsulations in dendrimers and have explored their applications in drug delivery, light harvesting, confined nanoreactors, etc.[19] In the encapsulation process, guest molecules are captured in the cavities of the dendritic boxes when the dendrimers are constructed in the presence of the guest molecules. Diffusion of the locked-in guest molecules from the nanodimensional boxes into solution is very slow because of the close packing of the peripheral shell. Compared to the structurally perfect but synthetically tedious dendritic boxes, hyperbranched molecular containers have obvious synthetic advantages but have been rarely investigated.[20] We here utilize a novel fluorescence process to prove that our hyperbranched polymer can serve as a molecular container.

We have recently discovered an intriguing phenomenon of aggregation-induced emission (AIE) in silole and tetraphenylethene (TPE) as well as their derivatives. These molecules are nonemissive in solutions but become highly luminescent when aggregated or fabricated into solid films.[21] We have proved that the AIE effect stems from the restriction of intramolecular rotations, which blocks the nonradiative channel via rotational energy relaxation and effectively

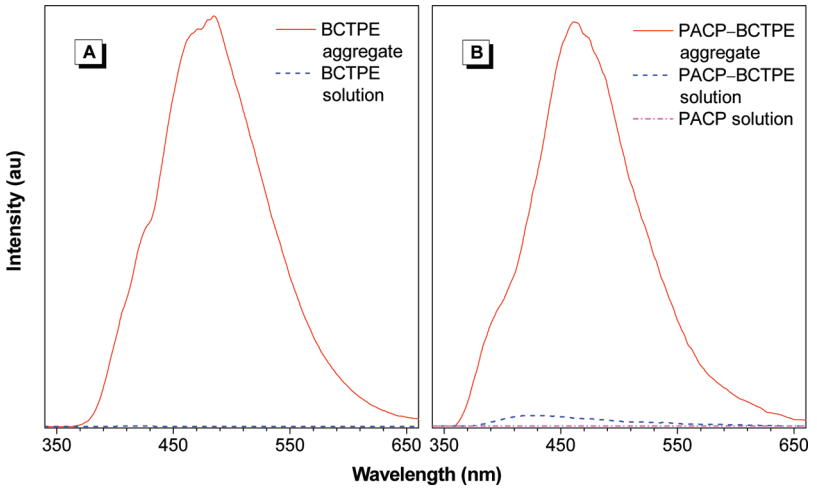

Figure 8. (A) Emission spectra of BCTPE in pure THF and a THF/H_2O (1/9 v/v) mixture. [BCTPE] = 0.3 mg/mL; λ_{ex} = 330 nm. (B) Emission spectra of PACP (sample taken from Table 1, no. 7) in THF and PACP−BCTPE (sample taken from Table 4, no. 6) in pure THF and a THF/hexane (1/9 v/v) mixture. [PACP−BCTPE] = 1 mg/mL; λ_{ex} = 280 nm (for PACP); λ_{ex} = 330 nm (for PACP−BCTPE).

Table 4. Polycyclotrimerizations of the ABP Monomer Catalyzed by Cp*Ru(PPh_3)$_2$Cl in the Presence of AIE Luminogen BCTPE[a]

no.	time (min)	$M_{w,r}$[b]	PDI[b]
1	5	2700	1.3
2	15	3500	1.5
3	30	4300	1.9
4	60	4800	2.0
5	120	9600	2.3
6	180	14600	3.0

[a] Carried out in THF under nitrogen at room temperature; $[M]_{ABP}$ = 0.1 M, $[M]_{ABP}/[M]_{BCTPE}$ = 25:1, [cat.] = 1 mM. [b] Estimated by GPC in THF on the basis of a linear polystyrene calibration.

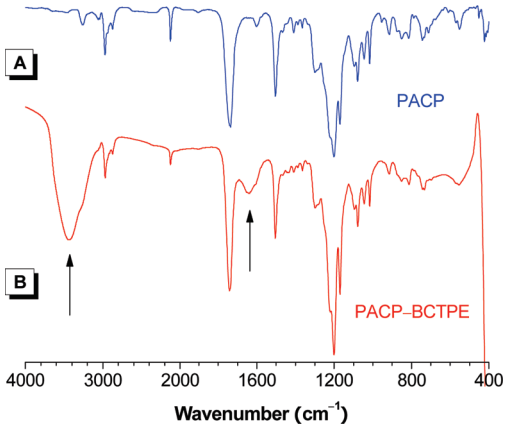

Figure 9. IR spectra of (A) pure PACP (sample taken from Table 1, no. 6) and (B) BCTPE-loaded PACP prepared by in situ polymerization (sample taken from Table 4, no. 6).

populates the radiative decay of the excitons. A wide variety of AIE-active luminogens have since been developed by our and other groups, examples of which include 1-cyano-*trans*-1,2-bis(4-methylbiphenyl)ethylene, *N*,*N*-bis(salicylidene)-*p*-phenylenediamine, bis-{4-[*N*-(1-naphthyl)phenylamino]phenyl}fumaronitrile, diphenyldistyrylbenzenes, tetraarylbutadienes, triarylethenes, and metalloles.[21−23]

The unique AIE effect inspires us to utilize AIE luminogens as probes to visualize internal cavities in our hyperbranched polymers. It is envisioned that the diyne polymerization in the presence of AIE dyes will lead to encapsulation of the dye molecules into the cavities of the hyperbranched polymers and that the trapped AIE dyes will become highly emissive when the cavities are shrunk. A TPE derivative named 1,2-bis(4-carboxylphenyl)-1,2-diphenylethene (BCTPE)[24] is employed as a model luminogen to illustrate this process, as shown in Scheme 4. BCTPE is a typical AIE luminogen: it does not luminesce when it is molecularly dissolved in THF but strongly emits when its molecules are aggregated or clustered in a THF/water mixture containing a large amount of water (90 vol %; Figure 8A).

We carried out an in situ polycyclotrimerization reaction of the diyne monomer in the presence of BCTPE at a feed ratio of 25:1 and obtained a polymer with $M_{w,r}$ and p values of 14 600 and 0.728, respectively (Table 4). The PACP−BCTPE is highly emissive in the solid state even after the polymer has been purified by several dissolution−precipitation cycles, whereas its dilute solution in THF is only weakly luminescent (Figure 8B). This indicates that the AIE molecules have indeed been trapped in the internal cavities of the PACP and that the free volumes in the cavities of the polymer are sufficiently large for the trapped BCTPE molecules to undergo intramolecular rotations. The AIE molecules cannot diffuse out from the internal cavities of the hyperbranched polymer, thanks to the hydrogen-bonding interaction between BCTPE and PACP (cf. Scheme 4). The existence of the hydrogen bonds in the PACP−BCTPE is manifested by the new absorption bands at 3436 and 1638 cm^{-1} in its IR spectrum (Figure 9).

The AIE process can be readily appreciated by visual observation. When the content of hexane in a THF/hexane mixture is smaller than 50%, PABP−BCTPE is almost nonluminescent; when the hexane content is higher than 50%, its emission becomes visible (Figure 10). The PABP−BCTPE molecules are aggregated in the solvent mixture with high hexane content because hexane is a poor solvent for both PACP and BCTPE. The visual observation is consistent with the spectral data shown in Figure 8B. In THF or a solvent mixture with a low content of a poor solvent (hexane or water), the PACP molecules take an extended conformation, which affords the AIE molecules enough free volumes to rotate within the polymer cavities. The AIE molecules cannot rotate freely in the shrunken cavities in a solvent mixture with a high content of hexane or water and hence become emissive. These experimental data provide solid evidence to prove that the PACP functions as a molecular container.

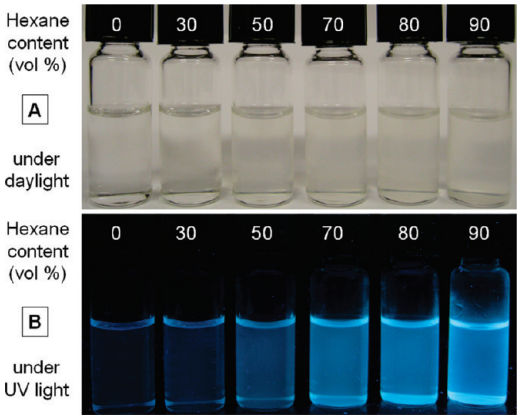

Figure 10. PACP−BCTPE (sample from Table 4, no. 6) in the THF/hexane mixtures with different volume fractions of hexane. Photographs taken under (A) room lighting and (B) UV illumination (365 nm). Sample concentration: 30 μg/mL.

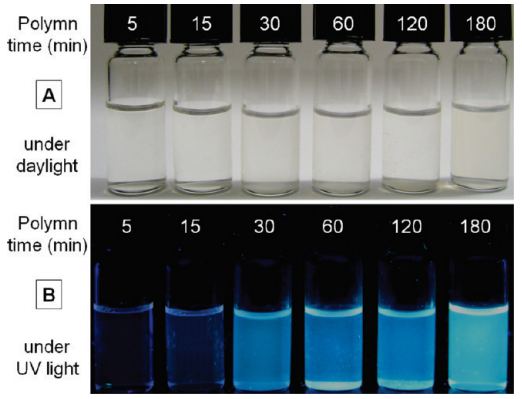

Figure 11. PACP−BCTPEs obtained from the in situ polymerization in different periods of time (cf. Table 4) in a THF/hexane mixture with 90% of hexane. Photographs taken under (A) room lighting and (B) UV illumination (365 nm). Sample concentration: 30 μg/mL.

To examine whether the AIE luminogen-trapping process is MW-dependent, we monitored the time course of the diyne polymerization in the presence of BCTPE. As can be seen from the polymerization results summarized in Table 4, the MW of the polymer is increased with an increase in the reaction time. When the polymerization time is shorter than 15 min, the MW of the resultant polymer is low and the polymer aggregates practically do not luminesce (Figure 11). When the polymerization time is longer than 30 min, the polymer aggregates show gradually enhanced emission with increasing MW. Evidently, when the MW of a polymer is not high enough, there exist few internal cavities but many defects in the topological structure of the polymer, which cannot capture sufficient amounts of the AIE molecules and hold them inside the polymer sphere. A high-MW polymer can encapsulate more AIE molecules, thus endowing its aggregates with efficient light emission.

Bursting Hydrolysis. The PACP synthesized in this work can be structurally viewed as a polyester, as it contains three ester groups in one repeat branch. The hyperbranched structure of the polyester allows water molecules and catalytic species, if any, to penetrate into the core of the polymer sphere. The PACP may thus undergo rapid hydrolysis in a bursting manner, causing the polymer skeleton to collapse abruptly and hence releasing the trapped AIE molecules like a bomb explodes (cf. Scheme 4). It has been generally difficult to monitor the hydrolysis process of a polyester

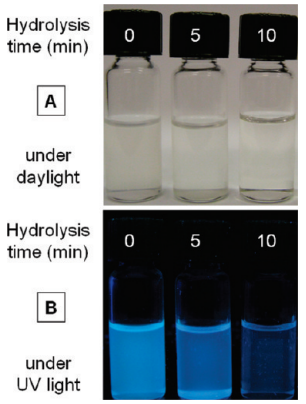

Figure 12. Hydrolysis products of PACP−BCTPEs obtained in different reaction times in a THF/hexane mixture containing 90% of hexane. Photographs taken under (A) room lighting and (B) UV illumination (365 nm). Sample concentration: 30 μg/mL.

because it is neither absorptive nor emissive, but the AIE characteristic of the BCTPE molecules encapsulated in the cavity of the hyperbranched polymer should make the job easier because the AIE luminogen can serve as a sensitive fluorescence probe or reporter.

While a conventional aromatic polyester with a linear molecular structure can take days to decompose, the hyperbranched aromatic polyester PACP is hydrolyzed in a time scale of minutes. After stirring at room temperature in THF in the presence of a catalytic amount of potassium hydroxide for 5 min, the $M_{w,r}$ of the PACP is decreased from 14 600 to 6200 with a slight narrowing in its PDI (from 3.0 to 2.1). Accompanying the hydrolysis, fluorescence intensity of the aggregates of the reaction products in the THF/hexane mixture (1:9 v/v) is weakened (Figure 12B). After 10 min reaction, the polymer is further hydrolyzed to very low-MW fragments that cannot even be precipitated out. As a result, the emission is further weakened. Evidently, the AIE luminogen has permitted a visual monitoring of the hydrolysis process of the polyester.

Spectroscopic analysis of the reaction mixture reveals that 1,2,4- and 1,3,5-benzenetricarboxylic acid and bisphenol A are the main hydrolysis products, as anticipated. In other words, the PACP polymer is sensitively decomposed by the base-catalyzed hydrolysis to its "building blocks". Concomitantly, the loaded AIE luminogenic molecules in the hyperbranched molecular container are rapidly released into the solution, like shrapnels emanating from an exploding cluster bomb. This attribute makes the PACP a promising candidate as a drug carrier for the development of targeted missile therapy. The quantitative investigation on the encapsulation of various guest molecules, including pharmaceutically and clinically important drugs used in the real world, into this hyperbranched molecular container and their release from its internal cavities is underway in our laboratories, and the results will be published in due course.

Concluding Remarks

In this work, a group of ruthenium complexes is, for the first time, developed into effective catalysts for diyne polycyclotrimerization. The late transition metal catalysts are highly functionality-tolerant. C**1** shows higher catalytic activity than C**2** because the sterically bulkier and electronically richer Cp* ring of the former makes the phosphine ligand dissociation easier and the oxidative cyclization faster. The high-valent Ru(III) and Ru(IV) complexes (C**3** and **4**) catalyze the diyne polycyclotrimerization via in situ generation of active Ru(II) species. Hyperbranched

polymer is obtained at lower p values, while soluble nanogels are formed at higher p values (>0.75). DB of the polymer is ~0.76, higher than those of the conventional hyperbranched polymers (DB ~ 0.5). The absolute MW of the polymer determined by LLS is much higher than its relative MW estimated by GPC, substantiating its globular conformation. The polymer is macroscopically processable, thermally stable, and optically transparent. The PACP functions as an excellent molecular container and undergoes a bursting hydrolysis reaction, as revealed by the AIE-active fluorescence probe. These remarkable attributes may enable the polymer to find an array of high-tech applications, especially in the area of controlled drug delivery.

Experimental Section

General Information. Toluene, dioxane, and THF were distilled in an atmosphere of nitrogen from sodium benzophenone ketyl immediately prior to use. DCM was distilled under nitrogen over calcium hydride. The ABP monomer and the Ru complexes were prepared as described below. DCC, DMAP, TsOH, bisphenol A, propiolic acid, and other chemicals and reagents were all purchased from Aldrich and used as received without further purification.

$M_{n,r}$, $M_{w,r}$, and PDI values of the polymers were estimated by GPC using a Waters Associates liquid chromatograph equipped with a Waters 515 HPLC pump, a set of Styragel columns (HT3, HT4, and HT6; molecular weight range 10^2-10^7), a column temperature controller, a Waters 486 wavelength-tunable UV−vis detector, a Waters 2414 differential refractometer, and a Waters 2475 fluorescence detector. The polymer solutions in THF (~2 mg/mL) were filtered through 0.45 μm PTFE syringe-type filters before being injected into the GPC system. THF was used as eluent at a flow rate of 1.0 mL/min. The column temperature was maintained at 40 °C, and the working wavelength of the UV−vis detector was set at 254 nm. A set of monodisperse polystyrene standards (Waters) covering the molecular weight range of 10^3-10^7 were used for the molecular weight calibration. $M_{W,a}$ values of the polymers were determined on a LLS spectrometer (ALV/DLS/SLS-5022F) equipped with a multi-τ digital time correlator (ALV5000) and a cylindrical 22 mW He−Ne laser (λ_0 = 632 nm, Uniphase) as light source. The dn/dC value at 632.8 nm was measured on a Jianke differential refractometer to be 0.274 mL/g in THF at 25 °C.

X-ray diffraction intensity data of the monomer were collected at 100 K on a Bruker-Nonius Smart Apex CCD diffractometer with graphite-monochromated Mo Kα radiation. The data were processed using the SAINT and SADABS routines, and the structure solution and refinement were carried out by the SHELXTL suite of X-ray programs (version 6.10). IR spectra were recorded on a Perkin-Elmer 16 PC FTIR spectrophotometer. ^{1}H, ^{13}C, and ^{1}H{^{13}C} HSQC NMR spectra were measured on Bruker ARX 300 or 400 NMR spectrometers using chloroform-d or DCM-d_2 as solvent. Optical transmission spectra were measured on a Milton Ray Spectronic 3000 array spectrophotometer. Mass spectra were recorded on a GCT Premier CAB 048 mass spectrometer. TGA measurements were conducted under nitrogen and in air on a Perkin-Elmer TGA 7 analyzer at a heating rate of 20 °C/min.

Monomer Synthesis. 4,4′-Isopropylidenediphenyl bipropiolate monomer was prepared according to the synthetic routes given in Scheme 2.[25] A detailed experimental procedure for the monomer preparation is given below.

In a 500 mL round-bottom flask were dissolved 3.42 g (15 mmol) of bisphenol A, 6.81 g (33 mmol) of DCC, 0.57 g (3 mmol) of TsOH, and 0.37 g (3 mmol) of DMAP in 240 mL of DCM/THF (3:1 v/v) under nitrogen. The solution was cooled to 0 °C with an ice−water bath, into which 2.2 g (31.5 mmol) of propiolic acid dissolved in 12 mL of DCM/THF was added under stirring via a dropping funnel. The reaction mixture was stirred overnight.

Scheme 5

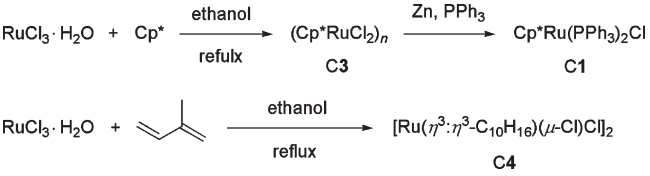

After filtering out the formed urea solid, the solution was concentrated by a rotary evaporator. The crude product was purified by a silica gel column using chloroform/hexane (1:3 v/v) as eluent. Recrystallization in a chloroform/hexane mixture (1:1 v/v) gave 3.05 g of solid product. Yield: 61.2%. IR (thin film) (ν, cm^{-1}): 3268 (≡C−H stretching), 2126 (C≡C stretching), 1731 (C=O stretching). ^{1}H NMR (400 MHz, CD_2Cl_2), δ (TMS, ppm): 7.26 [d, J (H,H) = 8.4 Hz, 4H, aromatic protons meta to O], 7.04 [d, J (H,H) = 8.4 Hz, 4H, aromatic protons ortho to O], 3.14 (s, 2H, ≡C−H), 1.68 (s, 6H, CH3). ^{13}C NMR (100 MHz, CD_2Cl_2), δ (TMS, ppm): 151.6, 149.3, 148.3, 128.6, 121.3, 77.2, 74.7, 43.1, 31.1. HRMS (EI): m/e 332.0885 (calcd 332.1049).

Catalyst Preparation. $CpRu(PPh_3)_2Cl$ (C**2**) complex was prepared following previously published procedures,[11] while Ru complexes C**1**, C**3**, and C**4** were synthesized according to the synthetic routes shown in Scheme 5. The detailed experimental procedures for the preparation of these complexes are described below.

*[Cp*RuCl$_2$]$_n$ (C3).* Into a two-necked round-bottomed flask equipped with a condenser was added 1.5 g (6.6 mol) of $RuCl_3 \cdot H_2O$. The flask was put under vacuum for 1 h and then refilled with dry nitrogen. Afterward, 25 mL of deoxygenated ethanol and 2.25 g (16.5 mmol) of pentamethylcyclopentadiene were injected into the flask under stirring. After refluxing for 3 h, the dark brown crude product was collected on a Buchner funnel and washed with 5 mL of ethanol and 5 mL of dry diethyl ether two times. Drying under vacuum gave complex C**3** in 60.8% yield. ^{1}H NMR (400 MHz, $CDCl_3$), δ (TMS, ppm): 4.63 (broad, CH_3).

*Cp*Ru(PPh$_3$)$_2$Cl (C1).* Into a two-necked round-bottomed flask was added 160 mg of [Cp*RuCl$_2$]$_n$ and 250 mg of zinc powder. The flask was vacuumed for 1 h and refilled with nitrogen. Afterward, 20 mL of deoxygenated ethanol was injected into the flask under stirring. After the solution color had changed to green, 530 mg of PPh_3 was added. The solution color gradually turned from green to yellow. After stirring for 24 h, the zinc powder was filtered and the filtrate was concentrated. Upon addition of 20 mL of diethyl ether, C**1** was precipitated out, while the unreacted PPh_3 remained dissolved. After washing with diethyl ether three times, the precipitate was collected and dried under vacuum. Yield: 56.3%. ^{1}H NMR (300 MHz, C_6D_6), δ (TMS, ppm): 6.8−8.3 (m, 30H, Ar−H), 1.15 (s, 15H, CH_3). ^{31}P NMR (C_6D_6), δ (PPh_3, ppm): 38.8 (s, Ru−PPh_3).

[Ru(η^3:η^3-C$_{10}$H$_{16}$)(μ-Cl)Cl]$_2$ (C4). Into a solution of $RuCl_3 \cdot H_2O$ (1.1 g) in 20 mL of ethanol was added 50 mL of isoprene, and the resultant mixture was refluxed under nitrogen for 18 h. The purple precipitate formed was collected on a Buchner funnel. After washing with ethanol and diethyl ether, the solid was dried under vacuum. Yield: 69.7%. Its characterization data matched with those reported in the literature.[13]

Polymerization Reaction. All the polymerization reactions were carried out under nitrogen using the standard Schlenk technique in a vacuum line system or an inert atmosphere glovebox. Typical experimental procedures for the polycyclotrimerization reaction of the ABP monomer using C**1** as the catalyst are described below.

To a 15 mL Schlenk tube with a three-way stopcock on the side arm was placed 2.4 mg (0.003 mmol) of C**1** under nitrogen in a glovebox. Freshly distilled THF (2.0 mL) was then injected into the tube using a hypodermic syringe. After stirring for

5 min, a solution of 100 mg (0.30 mmol) of the ABP monomer in 1.0 mL of THF was injected. The resultant mixture was stirred at room temperature under nitrogen for 2 h. The polymerization was quenched by the addition of a small amount of methanol. The solution was then added dropwise to 300 mL of hexane via a cotton filter under stirring. The precipitate was allowed to stand overnight and then collected by filtration. The polymer was washed with hexane and dried under vacuum at room temperature to a constant weight. Gray powder of PACP was obtained in 83.2% yield. $M_{w,r}$ 12 100; PDI 2.5 (Table 1, No. 6). IR (thin film), ν (cm^{-1}): 3259 (≡C−H stretching), 2124 (C≡C stretching), 1736 (C=O stretching). ^{1}H NMR (400 MHz, CD_2Cl_2), δ (TMS, ppm): 9.17 ($Ar_{1,3,5}$−H), (8.77, 8.46, 8.05) ($Ar_{1,2,4}$−H), 6.70−7.70 (original Ar−H), 3.14 (≡C−H), 1.71 (CH_3). ^{13}C NMR (100 MHz, CD_2Cl_2), δ (TMS, ppm): 168−163, 152−148, 138−120, 77.2, 74.7, 43.2, 31.2.

Using the similar procedures, the BCTPE-loaded PACPs (or PACP−BCTPEs) were prepared by the in situ polymerization reactions of the ABP monomer in the presence of the AIE luminogen BCTPE at a feed ratio 25:1 for specified periods of time.

Polymer Hydrolysis. The hydrolysis of the polyester (sample taken from Table 1, no. 6) was carried out in air. To a 10 mL test tube was placed 30 mg of the polymer. Freshly distilled THF (2.6 mL) was injected into the tube using a hypodermic syringe. After stirring for 2 min, a solution of 300 mg of potassium hydroxide in 0.4 mL of water was injected. The resultant mixture was stirred at room temperature for 2 h. The hydrolysis products were mainly 1,2,4/1,3,5-benzenetricarboxylic acids and bisphenol A. The molar ratio between 1,2,4- and 1,3,5-benzenetricarboxylic acids was found to be 4:1 by integrating the resonance peaks of the protons of the benzene rings ($A_{1,2,4}/A_{1,3,5}$ = 4:1), consistent with the $F_{1,2,4}$ ratio (~80%) of the starting polymer (cf. Table 3, no. 4).

Characterization Data for the Hydrolysis Products. Solid; yield 81.7%. ^{1}H NMR (400 MHz, 2 M KOH in D_2O), δ (TMS, ppm): 8.29 (s, $Ar_{1,3,5}$−H of benzenetricarboxylic acid), 7.81 (s, $Ar_{1,2,4}$−H of benzenetricarboxylic acid), 7.74 [d, J (H,H) = 8.0 Hz, $Ar_{1,2,4}$−H of benzenetricarboxylic acid], 7.39 [d, J (H,H) = 8.0 Hz, $Ar_{1,2,4}$−H], 6.95 [d, J (H,H) = 6.8 Hz, aromatic protons meta to O of bisphenol A], 6.41 [d, J (H,H) = 6.8 Hz, aromatic protons ortho to O of bisphenol A], 1.43 (s, CH_3). ^{13}C NMR (100 MHz, CD_2Cl_2), δ (TMS, ppm): (1,2,4- and 1,3,5-benzenetricarboxylic acid) 177.0, 176.5, 174.3, 174.2, 140.3, 137.0, 136.5, 136.2, 131.2, 129.8, 127.4, 126.7 (bisphenol A), 163.3, 137.5, 127.5, 117.8, 40.1, 30.3.

Model Reaction. Cyclotrimerizations of methyl propiolate were carried out as model reactions. The procedures were similar to those described above for the polycyclotrimerization reactions. The crude products trimethyl 1,2,4- and 1,3,5-benzenetricarboxylates were separated and purified by silica gel column chromatography using chloroform/hexane mixture (1:4 v/v) as eluent. The total isolation yields and the molar ratios of 1,2,4- to 1,3,5-isomers obtained by different catalysts are summarized in Table 3.

Characterization Data for Model Compound. Colorless solid; yield 87.3% (Table 3, no. 1). ^{1}H NMR (400 MHz, $CDCl_3$), δ (TMS, ppm): 8.84 (s, $Ar_{1,3,5}$−H), [8.41 (s); 8.19 (d), J (H,H) = 8.2 Hz; 7.74 (d), J (H,H) = 8.0 Hz,] ($Ar_{1,2,4}$−H), 3.95 (m, CH_3). ^{13}C NMR (100 MHz, CD_2Cl_2), δ (TMS, ppm): 167.6, 166.8, 165.4, 165.3, 136.2, 134.6, 132.4, 132.2, 131.6, 131.2, 130.2, 128.9, 52.8 (m). HRMS (EI): m/e 253.0699 [$(M + 1)^+$, calcd 253.0634].

Acknowledgment. We are grateful to Profs. Chi Wu and To Ngai of The Chinese University of Hong Kong for their technical assistance and helpful discussions. This work was partially supported by the Research Grants Council of Hong Kong (603509 and 602707), the National Science Foundation of China (20634020), and the Ministry of Science & Technology of China (2009CB623605). B.Z.T. thanks the support from the Cao Guangbiao Foundation of Zhejiang University.

Supporting Information Available: Table giving the crystal analysis data of the monomer and figure showing the TGA curves of the polymer in air and under nitrogen. This material is available free of charge via the Internet at http://pubs.acs.org.

References and Notes

(1) For examples of general reviews on hyperbranched polymers, see: (a) Gao, C.; Yan, D. *Prog. Polym. Sci.* **2004**, *29*, 183. (b) Tomalia, D. A.; Fréchet, J. M. *J. Polym. Sci., Part A: Polym. Chem.* **2002**, *40*, 2719. (c) Jikei, M.; Kakimoto, M. *Prog. Polym. Sci.* **2001**, *26*, 1233. (d) Voit, B. *J. Polym. Sci., Part A: Polym. Chem.* **2000**, *38*, 2505. (e) Pattern, T. E.; Matyjaszewski, K. *Adv. Mater.* **1998**, *10*, 901.

(2) For examples of reviews about our research program on hyperbranched polymers, see: (a) Liu, J.; Lam, J. W. Y.; Tang, B. Z. *Chem. Rev.* **2009**, *109*, DOI: 10.1021/cr900149d. (b) Haussler, M.; Tang, B. Z. *Adv. Polym. Sci.* **2007**, *209*, 1. (c) Haussler, M.; Lam, J. W. Y.; Zheng, Y.; Peng, H.; Luo, J.; Chen, J.; Law, C. C. W.; Tang, B. Z. *C. R. Chim.* **2003**, *196*, 289.

(3) Liu, J.; Zheng, R.; Tang, Y.; Haussler, M.; Lam, J. W. Y.; Qin, A.; Ye, M.; Hong, Y.; Gao, P.; Tang, B. Z. *Macromolecules* **2007**, *40*, 7473.

(4) (a) Irzhak, T. F.; Irzhak, V. I.; Malkov, G. V.; Estrin, Ya. I.; Badamshina, E. R. *J. Polym. Sci., Ser. A* **2008**, *50*, 74. (b) Irzhak, T. F.; Irzhak, V. I.; Malkov, G. V.; Estrin, Ya. I.; Badamshina, E. R. *J. Polym. Sci., Ser. B* **2009**, *51*, 183.

(5) Zheng, R.; Häussler, M.; Dong, H.; Lam, J. W. Y.; Tang, B. Z. *Macromolecules* **2006**, *39*, 7973.

(6) (a) Haussler, M.; Qin, A.; Tang, B. Z. *Polymer* **2007**, *48*, 6181. (b) Zheng, R.; Dong, H. C.; Tang, B. Z. In *Macromolecules Containing Metal- and Metal-like Elements*; Abd-El-Aziz, A., Carraher, C., Pittman, C., Sheats, J., Zeldin, M., Eds.; Wiley: New York, 2005; Vol. *4*, Chapter 2, pp 7−36.

(7) Haussler, M.; Liu, J. Z.; Zheng, R.; Tang, B. Z. *Macromolecules* **2007**, *40*, 1914.

(8) (a) Saito, S.; Yamamoto, Y. *Chem. Rev.* **2000**, *100*, 2901. (b) Yamamoto, Y. *Curr. Org. Chem.* **2005**, *9*, 503.

(9) (a) Kirchner, K.; Calhorda, M. J.; Schmid, R.; Veiros, L. F. *J. Am. Chem. Soc.* **2003**, *125*, 11721. (b) Cadierno, V.; Garcia-Garrido, S. E.; Gimeno, J. *J. Am. Chem. Soc.* **2006**, *128*, 15094.

(10) Lindner, E.; Haustein, M.; Mayer, H. A.; Gierling, K.; Fawzi, R.; Steimann, M. *Organometallics* **1995**, *14*, 2246.

(11) Bruce, M. I.; Hameister, C.; Swincer, A. G.; Wallis, R. C. *Inorg. Synth.* **1990**, *28*, 270.

(12) Oshima, N.; Suzuki, H.; Moro-oka, Y. *Chem. Lett.* **1984**, 1161.

(13) Cox, D. N.; Roulet, R. *Inorg. Chem.* **1990**, *29*, 1360.

(14) (a) Gemel, C.; LaPensee, A.; Mauthner, K.; Mereiter, K.; Schmid, R.; Kirchner, K. *Monatsh. Chem.* **1997**, *128*, 1189–1199. (b) Ernst, C.; Walter, O.; Dinjus, E. *J. Prakt. Chem.* **1999**, *341*, 801.

(15) Albers, M. O.; de Waal, D. J. A.; Liles, D. C.; Robinson, D. J.; Singleton, E.; Wiege, M. B. *J. Chem. Soc., Chem. Commun.* **1986**, 1680.

(16) (a) Otsuka, E.; Kurumada, K.; Suzuki, A.; Matsuzawa, S.; Takeuchi, K. *J. Sol-Gel Sci. Technol.* **2008**, *46*, 71. (b) Chu, J. B.; Huang, S. M.; Zhu, H. B.; Xu, X. B.; Sun, Z.; Chen, Y. W.; Huang, F. Q. *J. Non-Cryst. Solids* **2008**, *354*, 5480.

(17) Funke, W.; Okay, O.; Joos-Muller, B. *Adv. Polym. Sci.* **1998**, *136*, 139.

(18) (a) Hawker, C. J.; Malmstrom, E. E.; Curtis, W. F.; Kampf, J. P. *J. Am. Chem. Soc.* **1997**, *119*, 9903. (b) Harth, E. M.; Hecht, S.; Helms, B.; Malmstrom, E. E.; Frechet, J. M. J.; Hawker, C. J. *J. Am. Chem. Soc.* **2002**, *124*, 3926.

(19) (a) Jansen, J.; de Brabander-van den Berg, E. M.; Meijer, E. W. *Science* **1994**, *266*, 1226. (b) Gorman, C. B.; Smith, J. C. *Acc. Chem. Res.* **2001**, *34*, 60. (c) Crooks, R. M.; Zhao, M.; Sun, L.; Chechik, V.; Yeung, L. K. *Acc. Chem. Res.* **2001**, *34*, 181. (d) Vogtle, F.; Gestermann, S.; Hesse, R.; Schwierz, H.; Windisch, B. *Prog. Polym. Sci.* **2000**, *25*, 987. (e) Aulenta, F.; Hayes, W.; Rannard, S. *Eur. Polym. J.* **2003**, *39*, 1741. (f) Stiriba, S.; Frey, H.; Haag, R. *Angew. Chem., Int. Ed.* **2002**, *41*, 1329.

(20) (a) Fu, Y.; Van Oosterwijck, C.; Vandendriessche, A.; Kowalczuk-Bleja, A.; Zhang, X.; Dworak, A.; Dehaen, W.; Smet, M. *Macromolecules* **2008**, *41*, 2388. (b) Shu, C. F.; Leu, C. M. *Macromolecules*

1999, *32*, 100. (c) Sunder, A.; Kramer, M.; Hanselmann, R.; Mülhaupt, R.; Frey, H. *Angew. Chem., Int. Ed.* **1999**, *38*, 3552.

(21) For examples of recent reviews, see: (a) Hong, Y. N.; Lam, J. W. Y.; Tang, B. Z. *Chem. Commun.* **2009**, 4332. (b) Liu, J.; J. W., Y.; Tang, B. Z. *J. Inorg. Organomet. Polym. Mater.* **2009**, *19*, 249. (c) Qian, L.; Zhi, J.; Tong, B.; Yang, F.; Zhao, W.; Dong, Y. *Prog. Chem.* **2008**, *20*, 673.

(22) (a) Luo, J. D.; Xie, Z. L.; Lam, J. W. Y.; Cheng, L.; Chen, H. Y.; Qiu, C. F.; Kwok, H. S.; Zhan, X. W.; Liu, Y. Q.; Zhu, D. B.; Tang, B. Z. *Chem. Commun.* **2001**, 1740. (b) Chen, J.; Law, C. W.; Lam, J. W. Y.; Dong, Y.; Lo, S. M. F.; Williams, I. D.; Zhu, D.; Tang, B. Z. *Chem. Mater.* **2003**, *15*, 1535. (c) Hong, Y. N.; Haussler, M.; Lam, J. W. Y.; Li, Z.; Sin, K. K.; Dong, Y. Q.; Tong, H.; Liu, J. Z.; Qin, A. J.; Renneberg, R.; Tang, B. Z. *Chem.−Eur. J.* **2008**, *14*, 6428. (d) Li, Z.; Dong, Y. Q.; Lam, J. W. Y.; Sun, J. X.; Qin, A. J.; Haussler, M.; Dong, Y. P.; Sung, H. H. Y.; Williams, I. D.; Kwok, H. S.; Tang, B. Z. *Adv. Funct. Mater.* **2009**, *19*, 905.(e) Zhao, Z.; Wang, Z.; Lu, P.; Chan, C. Y. K.; Liu, D.; Lam, J. W. Y.; Sung, H. H. Y.; Williams, I. D.; Ma, Y.; Tang, B. Z. *Angew. Chem., Int. Ed.* **2009**, *48*, DOI: 10.1002/anie.200903698.

(23) (a) An, B.-K.; Kwon, S.-K.; Jung, S.-D.; Park, S. Y. *J. Am. Chem. Soc.* **2002**, *124*, 14410. (b) Yeh, H. C.; Yeh, S. J.; Chen, C. T. *Chem. Commun.* **2003**, 2632. (c) Chen, J.; Xu, B.; Ouyang, X.; Tang, B. Z.; Cao, Y. *J. Phys. Chem. A* **2004**, *108*, 7522. (d) Toal, S. J.; Jones, K. A.; Magde, D.; Trogler, W. C. *J. Am. Chem. Soc.* **2005**, *127*, 11661. (e) Wang, Z.; Shao, H.; Ye, J.; Tang, L.; Lu, P. *J. Phys. Chem. B* **2005**, *109*, 19627. (f) Yu, G.; Yin, S.; Liu, Y. Q.; Chen, J.; Xu, X.; Sun, X.; Ma, D.; Zhan, X.; Peng, Q.; Shuai, Z. G.; Tang, B. Z.; Zhu, D. B.; Fang, W.; Luo, Y. *J. Am. Chem. Soc.* **2005**, *127*, 6335. (g) Itami, K.; Yoshida, J. *Bull. Chem. Soc. Jpn.* **2006**, *79*, 811–824. (h) Han, M. R.; Hirayama, Y.; Hara, M. *Chem. Mater.* **2006**, *18*, 2784. (i) Bhongale, C. J.; Hsu, C.-S. *Angew. Chem., Int. Ed.* **2006**, *45*, 1404. (j) Kim, S.; Zheng, Q.; He, G. S.; Bharali, D. J.; Pudavar, H. E.; Baev, A.; Prasad, P. N. *Adv. Funct. Mater.* **2006**, *16*, 2317. (k) Peng, Q.; Yi, Y.; Shuai, Z.; Shao, J. *J. Chem. Phys.* **2007**, *126*, 114302. (l) Li, Y.; Li, F.; Zhang, H.; Xie, Z.; Xie, W.; Xu, H.; Li, B.; Shen, F.; Ye, L.; Hanif, M.; Ma, D.; Ma, Y. *Chem. Commun.* **2007**, 231. (m) Liu, Y.; Tao, X.; Wang, F.; Shi, J.; Sun, J.; Yu, W.; Ren, Y.; Zou, D.; Jiang, M. *J. Phys. Chem. C* **2007**, *111*, 6544. (n) Qian, Y.; Li, S.; Zhang, G.; Wang, Q.; Wang, S.; Xu, H.; Li, C.; Li, Y.; Yang, G. *J. Phys. Chem. B* **2007**, *111*, 5861. (o) Li, C.; Liu, X.; Yuan, M.; Li, J.; Guo, Y.; Xu, J.; Zhu, M.; Lv, J.; Liu, H.; Li, Y. *Langmuir* **2007**, *23*, 6754. (p) Shiraishi, K.; Kashiwabara, T.; Sanji, T.; Tanaka, M. *New J. Chem.* **2009**, *33*, 1680. (q) Zheng, Y.; Hu, Y. *J. Org. Chem.* **2009**, *74*, 5660. (r) Yang, Z.; Chi, Z.; Yu, T.; Zhang, X.; Chen, M.; Xu, B.; Liu, S.; Zhang, Y.; Xu, J. *J. Mater. Chem.* **2009**, *19*, 5541. (s) He, J.; Xu, B.; Chen, F.; Xia, H.; Li, K.; Ye, L.; Tian, W. *J. Phys. Chem. C* **2009**, *113*, 9892. (t) Wang, M.; Zhang, D.; Zhang, G.; Zhu, D. *Chem. Phys. Lett.* **2009**, *475*, 1. (u) Iida, A.; Yamaguchi, S. *Chem. Commun.* **2009**, 3002. (v) Shimizu, M.; Takeda, Y.; Higashi, M.; Hiyama, T. *Angew. Chem., Int. Ed.* **2009**, *48*, 3653.

(24) Xing, C. M.; Hong, Y. N.; Dong, Y. Q.; Lam, J. W. Y.; Qin, A. J.; Haussler, M.; Tang, B. Z. *Polym. Prepr.* **2007**, *48*, 466.

(25) Lam, J. W. Y.; Luo, J.; Dong, Y.; Cheuk, K. K. L.; Tang, B. Z. *Macromolecules* **2002**, *35*, 8288.